On the Systematic Occurrence of Compound Cold Spells in North America and Wet or Windy Extremes in Europe

Gabriele Messori, Davide Faranda

On the Systematic Occurrence of Compound Cold Spells in North America and Wet or Windy Extremes in Europe

Gabriele Messori[1,2] Davide Faranda[3,4,5]

1. Department of Earth Sciences and Centre of Natural Hazards and Disaster Science (CNDS), Uppsala University, Uppsala, Sweden.
2. Department of Meteorology and Bolin Centre for Climate Research, Stockholm University, Stockholm, Sweden.
3. Laboratoire des Sciences du Climat et de l'Environnement, LSCE/IPSL, CEA-CNRS-UVSQ, Université Paris-Saclay, Gif-sur-Yvette, France.
4. London Mathematical Laboratory, London, UK.
5. LMD/IPSL, École Normale Supérieure, PSL research University, Paris, France.

Corresponding author: Gabriele Messori (gabriele.messori@geo.uu.se)

Key Points:

- North American cold spells and European wet or windy extremes are very strongly coupled to recurrent large-scale atmospheric patterns.
- The compound occurrence of North American cold spells and European wet or windy extremes is associated with common atmospheric patterns.
- These compound extremes show weaker evidence of common atmospheric patterns than all temperature, precipitation and wind anomalies.

Abstract

The repeated co-occurrence of cold spells over Eastern North America and wet or windy extremes over Western Continental Europe during recent winters, has led to hypothesise a link between the two. Here, we analyse the interplay between the large-scale atmospheric circulation and co-occurring cold spells in North America and wet or windy extremes in Europe. We collectively term these occurrences compound cold–wet–windy extremes. We leverage a recent approach grounded in dynamical systems theory, which provides an analytically and computationally efficient analysis of spatially resolved, multivariate climate extremes. We find that there are specific, recurrent large-scale atmospheric circulation patterns systematically associated with both the individual extremes and co-occurring cold–wet–windy anomalies. Evidence for this is also found when focussing on compound cold–wet–windy extremes, although with a weaker signal. This motivates further analyses focussing specifically on the statistics and drivers of these compound extreme occurrences.

Plain Language Summary

In recent winters, very cold weather over the eastern part of North America and stormy weather or heavy rainfall in Europe have often made the news. One may think that these events are independent, since they occur several thousands of kilometres apart. However, researchers have hypothesised that there may be weather patterns that connect these different weather episodes. Here we test this idea. We find that there is indeed a connection between unusually cold weather in Eastern North America and unusually stormy weather and heavy rainfall in Western Continental Europe. We also find a link, albeit weaker, when focussing specifically on extreme events – namely only the coldest of the cold spells, the windiest of the stormy days and the wettest of the heavy rainfall days. The strongest connection, however, emerges when looking at unusual but not extreme weather episodes.

1 Introduction

During recent winters, ostensibly frequent cold spells in Eastern North America (ENA) and wet or windy extremes in Western Continental Europe (WCE) have garnered widespread scientific attention (e.g. Palmer 2014; Lee *et al.*, 2015; Matthias and Kretschmer, 2020; van Oldenborgh *et al.*, 2015; Hillier and Dixon, 2020; Owen *et al.*, 2021). These extremes have typically been discussed separately. However, their repeated co-occurrence suggests that they may be spatially compounding extremes, namely geographically remote extremes associated with common physical drivers. Specifically, Messori *et al.* (2016) argued for a link mediated by large-scale atmospheric circulation anomalies over the North Atlantic. However, extreme wet or windy weather in Europe was not explicitly investigated. Later, De Luca *et al.* (2020) focussed on co-occurring cold extremes in ENA and wet extremes in Europe, providing partial support for Messori *et al.* (2016). The study used an approach similar to the one we will adopt here, yet did not consider variables associated with the large-scale atmospheric circulation nor wind extremes. Most recently, Leeding *et al.* (2022) confirmed the repeated co-occurrence of cold spells in North America and wet or windy extremes in Europe, which we hereafter collectively term compound cold–wet–windy extremes, yet again highlighted the need for further analysis of the associated circulation patterns. The current understanding of these compound cold–wet–windy extremes is thus incomplete. Filling this knowledge gap is all the more urgent in view of the growing awareness of the relevance of compound extremes, whose impacts often exceed the sum of those due to the individual events comprising them (Lunt *et al.*, 2016; Zscheischler *et al.*, 2018).

The multivariate perspective inherent to compound extremes, adds complexity to conventional statistical tools for the study of extremes (Naveau, 2005). A wide range of approaches have been proposed to deal with multivariate extreme value statistics in climate data, from copula-based methods to max-stable models, conditional exceedance models, machine learning algorithms and more (*e.g.* Oesting and Stein, 2018; Brunner *et al.*, 2019; Tavakol *et al.*, 2020; Towler *et al.*, 2020; Vogel *et al.*, 2021). Spatially compounding extremes, such as the ones we consider here, present the additional challenge of how to incorporate spatial information into the analysis. Some of the above multivariate statistical approaches may be extended to incorporate spatial information, but this often results in highly complex models (e.g. Genton, 2015; Liu *et al.*, 2021).

Here, we leverage dynamical systems theory to provide an analytically and computationally efficient, spatially resolved analysis of compound cold–wet–windy extremes in ENA and WCE. The approach builds upon recent advances in dynamical systems theory (Faranda *et al.*, 2020a), and allows to compute the instantaneous coupling between different atmospheric variables, which we term *co-recurrence ratio*, or α. In this study, we extend this approach for the first time beyond the bivariate case. We propose this as an effective complement to existing analyses of spatially compounding extremes, which may support our understanding of the interplay between different climate extremes and their physical drivers.

We specifically seek to answer the following questions:

(i) Do cold spells over ENA and wet or windy extremes over WCE individually emerge as events with a particularly strong coupling to large-scale circulation patterns?

(ii) Is there evidence for recurrent large-scale circulation patterns systematically associated with the co-occurrence of these extremes?

Concerning the first question, there is a vast literature dealing with large-scale circulation patterns favouring the extremes analysed here (*e.g.* Haylock and Goodess, 2004; Cellitti *et al.*, 2006; Donat *et al.*, 2010; Grotjahn *et al.*, 2015; Harnik *et al.*, 2016; Smith and Sheridan, 2018; Laurila *et al.*, 2021). However, the question of whether the coupling of these extremes with the large-scale circulation is unusually strong relative to other days has not been addressed (with the exception of an exploratory analysis for North America in Faranda *et al.*, 2020a). Concerning the second question, both Messori *et al.* (2016) and Leeding *et al.* (2022) conditioned their large-scale atmospheric analysis only on cold spells in ENA, without explicitly accounting for the circulation associated with the European extremes. We begin by analysing separately North America and

Europe, and then explicitly address the spatially compounding nature of the cold–wet–windy extremes.

2 Data

We use ECMWF's ERA5 reanalysis data, over December–January–February (DJF) 1979–2020 and with a horizontal resolution of 0.5° (Hersbach *et al.*, 2020). We consider 2-metre temperature (t2m), 10-metre wind (10m wind), total precipitation (tp) and sea-level pressure (SLP). We chose SLP over geopotential height, as the latter displays long-term trends that could affect the dynamical systems analysis (Faranda *et al.*, 2020b). We compute daily averages from hourly data for surface variables and 6-hourly data for pressure-level variables. Anomalies are defined relative to a daily climatology smoothed using a 15-day running mean (similar to Harnik *et al.*, 2016). The 95th (5th for t2m) percentile of the local anomaly distributions is shown in Fig. S1.

The t2m in North America is analysed over 30–45 °N 260–290 °E (grey box in Fig. 1a), while 10-m wind and precipitation in Europe are analysed over 45–60 °N 350–20 °E (grey box in Fig. 2a). These domains approximately follow those used in Messori *et al.* (2016) for ENA cold spells and in Hanley and Caballero (2012) for WCE windstorms, respectively. The same domains are also used for analysing SLP co-recurrences (see Sect. 3). A sensitivity analysis using larger domains is presented in the Supplementary Material. Extreme events in t2m, 10m wind and tp are ranked according to the coldest, wettest or windiest anomalies, either at single gridboxes or averaged over the above analysis domains. Compound extremes are identified as described in Text S3. Unless otherwise specified, we analyse the 50 most extreme events. To avoid counting the same extreme multiple times, we impose a minimum separation of 5 days between successive events, following Messori *et al.* (2022). A similar minimum separation is imposed when selecting high α days..

Unless otherwise specified, we test statistical significance of composites by verifying whether at least 2/3 of composite members have the same sign. Assuming a binomial formula with equal chances for positive and negative anomalies, the probability of obtaining a greater than 2/3 sign agreement randomly is well below 5%.

3 Diagnosing the Coupling of Atmospheric Variables

Our analysis rests on computing the instantaneous coupling of multiple atmospheric variables, termed *co-recurrence ratio*, or α (Faranda *et al.*, 2020a; see also applications in De Luca *et al.*, 2020a,b and Messori and Faranda, 2021). Given two variables drawn from a chaotic dynamical system, α measures the extent to which recurrences in one variable correspond to recurrences in the other. For example, α computed for SLP and t2m over a given geographical domain diagnoses how often, given the recurrence of a specific t2m spatial pattern in the domain, one also observes the recurrence of the associated SLP spatial pattern. In other words, if α at a given timestep t in our dataset is large, then every time a t2m pattern similar to the t2m pattern of time t appears in the dataset (a *recurrence*), the SLP pattern at that other time will also resemble the SLP pattern of time t. This may then be interpreted as a high coupling. The converse holds for low α. The co-recurrence ratio may also be computed for more than two variables, and diagnoses the extent to which one observes simultaneous recurrences of all the variables being considered. When computing α for more than two variables, one is thus imposing additional constraints relative to the bivariate case. We therefore expect a trivariate α to display lower values than its bivariate counterpart.

Unlike other statistical coupling measures, α is instantaneous in time (local in phase space). Namely, a value of α is obtained for each timestep in the dataset being analysed. When computing α, the number of recurrences is always fixed to be the same for all variables; this makes α independent of the ordering of the variables, and it may thus not be interpreted in terms of causality. The range of the co-recurrence ratio is $0 \leq \alpha \leq 1$. We provide the details of the calculation of α for climate data in Text S1. All α values shown in the figures are anomalies, computed as described in Sect. 2. Distributions of these anomalies are shown in Fig. S2.

4 Large-scale drivers of cold spells in ENA and wet or windy extremes in WCE

4.1 Individual Extreme Event Classes

We first study separately cold spells in ENA and wet or windy extremes in WCE. To verify how these extremes couple to large-scale atmospheric patterns, we compute α between the relevant impact variable and SLP (Sect. 2). We begin by analysing days on which t2m in ENA is highly coupled to SLP. The 50 days with the highest coupling display an anomalous high pressure centred to the south-west of the Great Lakes region, flanked by two negative pressure anomaly cores (Fig.

1a; *cf.* Faranda *et al.*, 2020a). This tripole favours oceanic airmass advection and warm anomalies over Alaska, and simultaneous northerly advection of cold high-latitude air over central-eastern North America. Anomalies in excess of -10 K are attained over ENA, even though we are conditioning solely on α. The large-scale pattern is remarkably similar to that obtained by conditioning on the 50 coldest spells in ENA (Fig. S3a, Tab. S1), and resembles the spatial patterns found by previous studies investigating North American cold spells (*e.g.* Cellitti *et al.*, 2006; Messori *et al.*, 2016; Harnik *et al.*, 2016; Smith and Sheridan, 2018). Additionally, the 50 days with the highest coupling between SLP and t2m show an anomalously frequent occurrence of cold spells over a broad swath of North America (Fig. S4a), and a close overlap with the 50 coldest spells defined at each individual gridbox (not shown). Finally, we compute the $\alpha_{t2m,SLP}$ anomalies associated with the 50 coldest spells at each gridbox (Fig. 1b). The region that shows negative temperature anomalies in Figs. 1a, S3a also displays positive $\alpha_{t2m,SLP}$ anomalies in Fig. 1b. Thus, α shows that the cold spells share a similar spatial footprint and are systematically associated with a recurrent SLP configuration. We conclude that the occurrence of cold spells in ENA is systematically associated with a stronger than usual coupling between SLP and t2m. The qualitative results are not dependent on the choice of computing $\alpha_{t2m,SLP}$ by using the same geographical domain for both variables. Indeed, if we compute $\alpha_{t2m,SLP}$ using t2m over the cold spell box and the SLP pattern over a much larger North American domain, the results are qualitatively comparable (Fig. S5).

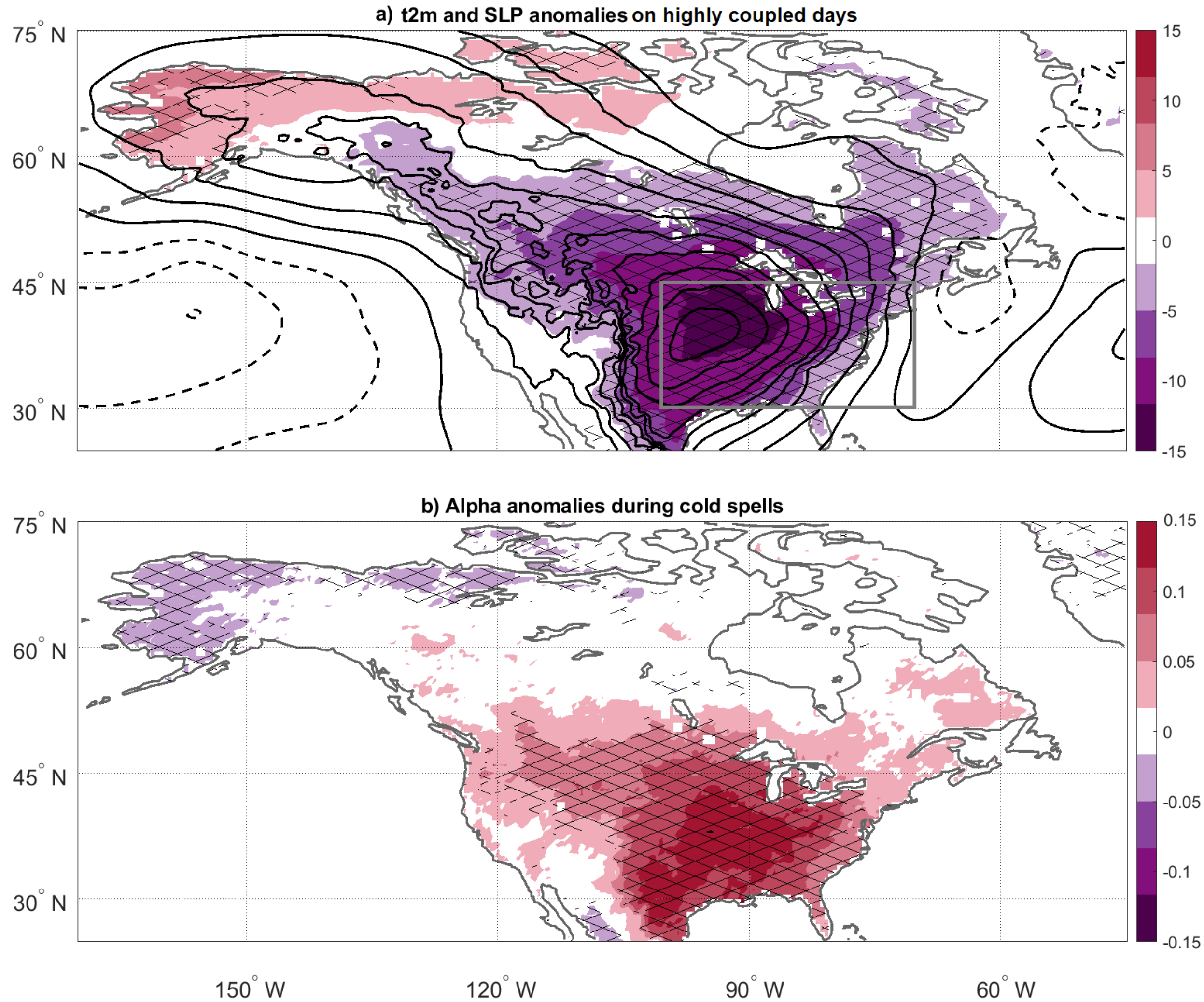

Figure 1. High t2m–SLP coupling days and cold spell days in ENA. Composite (a) t2m (K, colours) and SLP (hPa, contours) anomalies for the 50 days displaying the highest $\alpha_{t2m,SLP}$. (b) Composite $\alpha_{t2m,SLP}$ anomalies for the 50 coldest spells at each gridbox. SLP contours in (a) are every 2 hPa (negative dashed). Cross-hatching marks regions where at least two thirds of the (a) t2m and (b) $\alpha_{t2m,SLP}$ anomalies share the same sign. All α are computed over 30–45 °N, 260–290 °E (grey box in (a)).

We next shift the focus to 10m wind and tp anomalies in Europe. The 50 days with the highest coupling between 10m wind and SLP display strong positive 10m wind anomalies over WCE and an SLP anomaly dipole with a strong negative core to the south-east of Iceland and a weaker positive core over the western Mediterranean (Fig. 2a). This eastward-shifted, NAO-like dipole is typically associated with a zonalised and intensified jet stream, which in turn results in heightened cyclone frequency and wind destructiveness over Western Europe (Donat *et al.*, 2010; Hanley and Caballero, 2012; Gómara *et al.*, 2014; Messori and Caballero 2015; Messori *et al.*, 2019). A similar

SLP anomaly pattern, albeit with a northward-eastward shifted positive SLP core, is found for the 50 days with the highest coupling between tp and SLP (Fig. 2b). Because of the shift in the SLP core, the positive tp anomalies are also shifted slightly northwards relative to the 10m wind anomalies. We reconduct the geographical overlap between the 10m wind and tp anomalies to the dominant role of North Atlantic extratropical cyclones in bringing both strong winds and heavy precipitation to Western Europe, which in turn results in a close relationship between these two classes of extremes (Owen *et al.*, 2021). Indeed, De Luca *et al.*, 2020a explicitly showed that concurrent precipitation–wind extremes match high coupling days computed on precipitation and 10m wind over a large part of Western Europe. This relationship emerges here in the form of a high coupling between SLP patterns favouring the presence of cyclones over the continent (see references above) and large 10m wind and tp anomalies there. These SLP, tp and 10m wind anomaly patterns are additionally very similar to those conditioned on the occurrence of tp or 10m wind extremes in WCE (Fig. S3b, c, Tab. S1).

We moreover find that the 50 highest coupling days between SLP and the two impact variables correspond to an anomalously high occurrence of 10m wind and tp extremes over regions similar to those highlighted in Fig. 2a, b (Fig. S4b, c) and show a close overlap with the 50 most extreme 10m wind and tp events at each gridbox (not shown). The regions that show strong positive 10m wind and precipitation anomalies in Fig. 2a,b also display positive $\alpha_{10m\ wind,SLP}$ and $\alpha_{tp,SLP}$ anomalies during extremes in the former variables (Fig. 2c, d). In analogy with the cold spells analysis, we interpret this as meaning that the surface wind or precipitation extremes in WCE share common spatial footprints and are systematically associated with recurrent SLP configurations. These configurations are similar for the two classes of extremes. We conclude that the occurrence of wet or windy extremes in WCE is associated with a stronger than usual coupling between SLP and the relevant impact variable. Again, using a larger SLP domain for computing $\alpha_{10m\ wind,SLP}$ and $\alpha_{tp,SLP}$ provides qualitatively comparable results (Fig. S6).

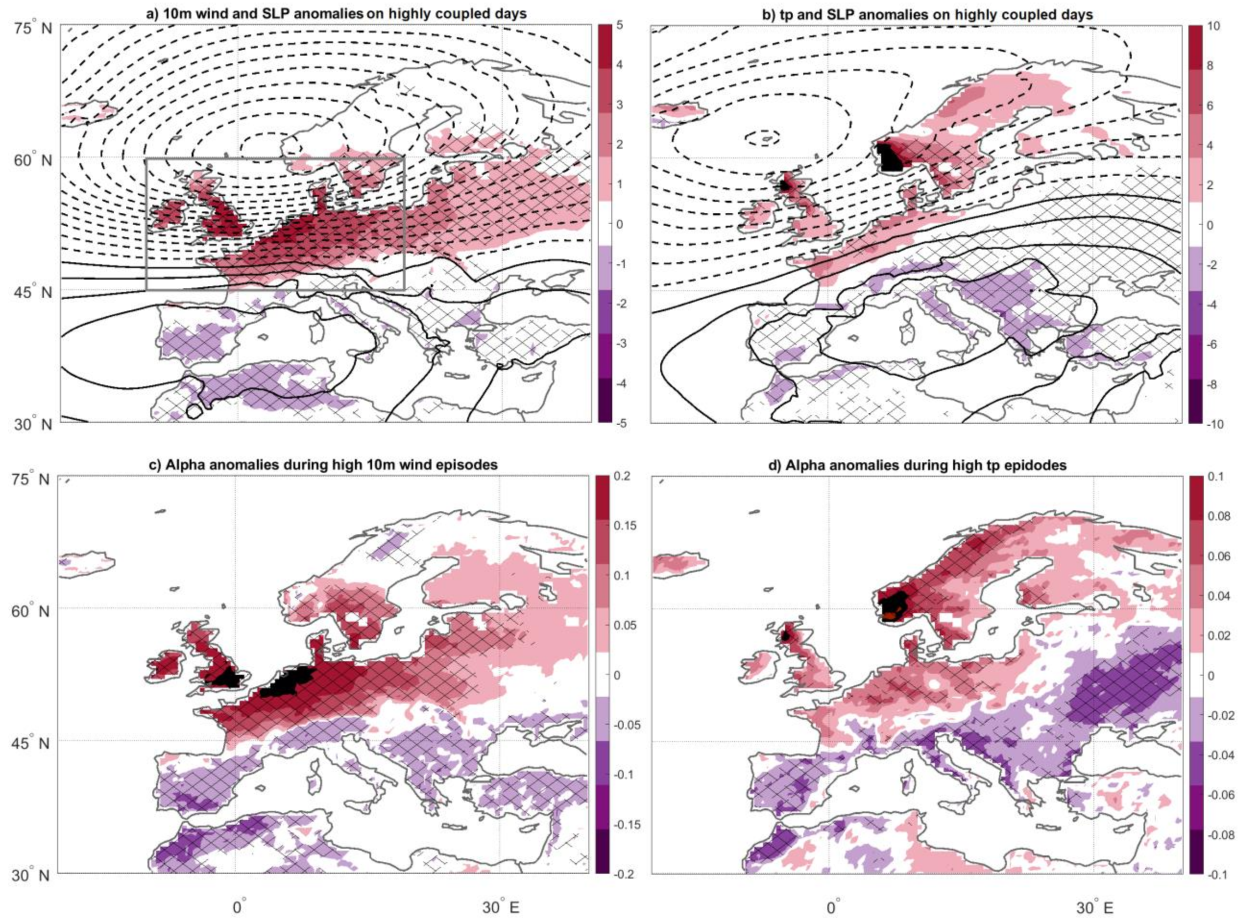

Figure 2. Days with high 10m wind or tp coupling with SLP and days with extreme 10m wind and tp in WCE. Composite (a)10m wind (m s^{-1}, colours) and SLP (hPa, contours) anomalies for the 50 days displaying the highest $\alpha_{10m\ wind,SLP}$ over WCE. (b) Same as (a) but for tp (mm day^{-1}) during the 50 days displaying the highest $\alpha_{tp,SLP}$. Composite (c) $\alpha_{10m\ wind,SLP}$ anomalies for the 50 most extreme 10m wind events at each gridbox. (d) Same as (c) but for $\alpha_{tp,SLP}$ and tp. SLP contours in (a, b) are every 2 hPa (negative dashed). Cross-hatching marks regions where at least two thirds of the anomalies shown in colours share the same sign. In Panel (b), days with no precipitation are not included in the latter calculation. The colour ranges in c, d differ; black shaded regions are beyond the colourbar limits. All α are computed over 45–60 °N, 350–20 °E (grey box in (a)).

4.2 Compound Cold–Wet–Windy Extremes

We next consider the link between the cold spells over ENA and the wet or windy extremes over WCE. In Sect. 4.1, we showed that the individual extreme classes display a close coupling of the relevant impact variable with the atmospheric circulation as diagnosed by SLP. If the North American and European extremes are indeed linked through a common large-scale circulation anomaly pattern, we would expect that both ENA cold spells and WCE wet or windy extremes should match high coupling events between the SLP patterns in the two continents. We thus compute α between North American and European SLP fields. For the 50 highest coupling days, both the SLP anomalies and the t2m, 10m wind and tp anomalies qualitatively match those discussed in Sect. 4.1 (*cf.* Fig. 3a, b with Figs. 1a and 2a, b). The most notable difference is the absence in Fig. 3a, b of weak negative SLP anomalies flanking the North American cold spells. However, the key SLP structures such as the anomalous high over central-eastern North America and the dipole over Europe are very closely reproduced. Similarly, the t2m, 10m wind and tp anomalies only show minor qualitative differences (*e.g.* in central-northern Canada), although they are systematically weaker in magnitude. The same qualitative picture holds if continental-scale domains are used to compute α between North American and European SLPs. However, the additional information given by the simultaneous enlargement of both the North American and European domains leads to the inclusion of SLP structures with little effect on the surface events of interests, and further dilutes the magnitude of the signal (Fig. S7a, b).

The high SLP coupling days between North America and Europe thus show a clear footprint in the surface anomalies. Moreover, the large-scale SLP patterns in Fig. 3a, b are comparable to those conditioned on the occurrence of the top 50 compound cold–wet–windy extremes (Text S3, Fig. S8). However, the link between the high SLP coupling days and the local extreme occurrences is weaker than what observed for the monovariate extremes. This is visible both when computing the occurrence of cold spells, 10m wind or tp extremes during the 50 highest SLP coupling days (*cf.* Figs. S4, S9) and when looking at composite coupling anomalies during the 50 coldest spells or most extreme tp or 10m wind events (*cf.* Figs. 1b, 2c, d and Fig. 3c, d). Specifically, the α anomalies shown in Fig. 3c, d show limited sign agreement, pointing to a large case-by-case variability. The link between the high SLP coupling days and compound cold–wet–windy extremes is generally stronger in WCE than in ENA, with the latter again showing limited sign agreement (Table S2).

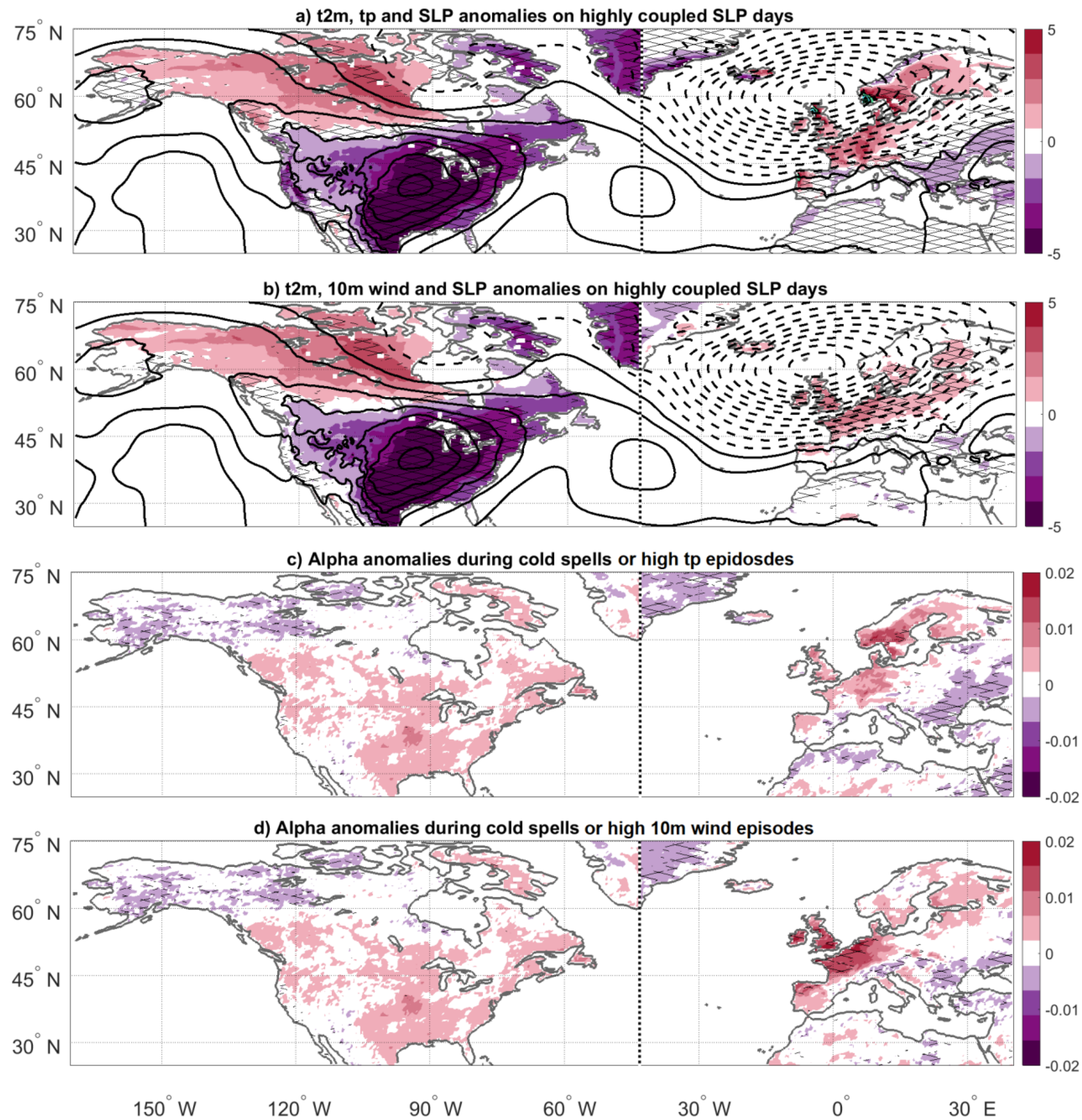

Figure 3. Days with high SLP coupling between North America and Europe and days with surface extremes. Composite (a) t2m (K, colours), tp (mm day^{-1}, colours) and SLP (hPa, contours) anomalies for the 50 days displaying the highest $\alpha_{SLP1,SLP2}$, where SLP1 is over 30–45 °N, 260–290 °E and SLP2 is over 45–60 °N, 350–20 °E. The t2m and tp are shown in the left and right-hand sides of the panel (separated by the vertical dotted line), respectively.(b) Same as (a) but for 10-metre wind (10m wind, m s^{-1}, colours) in the right-hand side of the panel. SLP contours in (a, b) are every 2 hPa (negative dashed). (c) Composite $\alpha_{SLP1,SLP2}$ anomalies for the 50 coldest spells or most extreme 10m wind events at each gridbox in the left and right-hand sides of the panel, respectively. (d) Same as (c) but for tp in the right-hand side of the panel. Cross-hatching marks regions where at least two thirds of the anomalies shown in colours share the same sign.

There is thus mixed evidence for the existence of co-recurrent pan-Atlantic circulation patterns coupled to the cold spells, 10m wind or tp extremes or the compound cold-wet-windy extremes analysed here. This may be due to α in Fig. 3 being based only on SLP and not including any of the impact variables. We thus compute the trivariate co-recurrence for pairs of our impact variables (t2m and tp and t2m and 10m wind, respectively) and SLP in the respective domains. With the trivariate coupling, we are requiring a co-recurrence of SLP patterns and surface variable patterns in two different variables over North American and European domains. The 50 highest trivariate coupling days display anomalies consistent with those in Fig. 3, albeit somewhat weakened (Fig. 4). The large-scale SLP patterns are comparable to those conditioned on the occurrence of compound cold–wet–windy extremes (Fig. S8). The link between the high-coupling days andboth classes of compound extremes in WCE again displays high sign agreement, while ENA shows high sign agreement only for compound cold–wet extremes (Table S2). A sensitivity test on broader SLP domains over both North America and Europe is shown in Fig. S10. We do not present here the alpha anomalies associated with extremes in single impact variable as we now consider more than one impact variable simultaneously in computing the coupling.

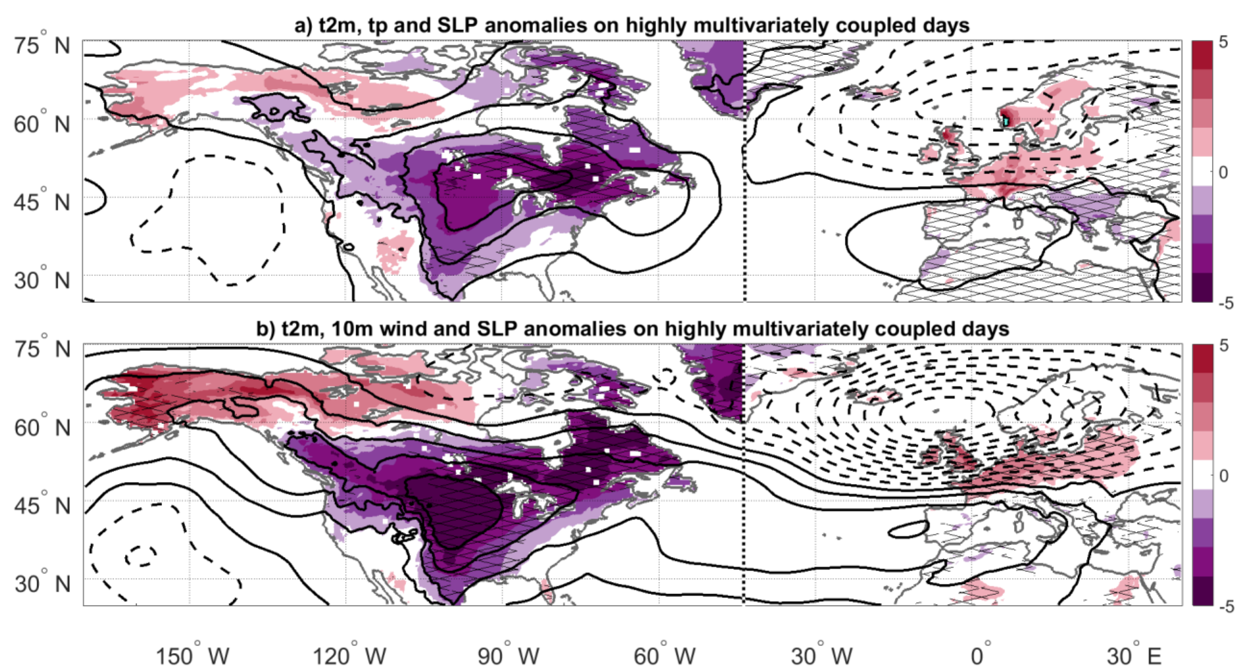

Figure 4. Days with high multivariate coupling between SLP and impact variables in North America and Europe. As Fig. 3 but for (a) $\alpha_{SLP,t2m,tp}$ and (b) $\alpha_{SLP,t2m,10m\ wind}$, where SLP is taken jointly over 30–45 °N, 260–290 °E and 45–60 °N, 350–20 °E and the impact variables are taken over the same domains as in Fig. 3.

5 Discussion and Conclusions

We studied the co-occurrence of cold spells in ENA and wet or windy extremes in WCE by computing the instantaneous coupling between multiple variables, termed *co-recurrence ratio*. It has previously been hypothesised that these extremes are statistically and physically linked (Messori *et al.*, 2016; De Luca *et al.*, 2020a; Leeding et al., 2022). In our analysis, we presented the first implementation of the co-recurrence ratio in a trivariate setting. We framed the study around two questions, namely: whether the individual extreme event classes of interest emerge as having a particularly strong coupling to large-scale atmospheric patterns; and whether there is evidence for recurrent large-scale circulation patterns linking the co-occurrence of these extremes in North America and Europe.

Both cold spells in ENA and wet or windy extremes in WCE show an unusually strong coupling to recurrent large-scale atmospheric patterns. Consistent with past literature, the key large-scale features are an anomalous ridge over central North America and an anomalous NAO-like dipole between the North Sea and the Mediterranean. Concerning the second question, our analysis suggests a nuanced picture. Days when the SLP patterns over ENA and WCE are strongly coupled display spatially coherent cold North American anomalies and wet or windy European anomalies, as well as a large-scale circulation resembling that individually associated with cold extremes in ENA and wet or windy extremes in WCE. Nonetheless, the link between the strongly coupled SLP days and extremes in both the individual impact variables we consider and compound extreme occurrences is moderate. Explicitly including the impact variables in the SLP coupling analysis, by computing a trivariate co-recurrence ratio does not markedly increase the link. The condition of co-recurring SLP patterns in ENA and WCE thus leads to a weaker connection to the surface extremes (or, conversely to a weaker connection between surface extremes and coupling anomalies) than in the analyses considering only one continent. Nonetheless, the days with a high trivariate co-recurrence ratio show an anomalously intense, zonal jet that Messori *et al.* (2016) and Leeding *et al.* (2022) hypothesised is key to connecting surface anomalies across the North Atlantic (Fig. S11). We thus conclude that cold ENA anomalies and wet or windy WCE anomalies are closely associated with common, recurrent large-scale atmospheric patterns grounded in a strong coupling between SLP fields over North America and Europe. The same holds to some extent for individual extreme event classes and for compound cold–wet–windy extremes, albeit with a weaker signal. A possible hypothesis is that synoptic-scale drivers which are only indirectly reflected in the large-scale picture – such as extratropical cyclones in the North Atlantic – may significantly modulate the occurrence of the extreme events.

Methodologically, our analysis provides a strong complement to more complex multivariate spatial extreme value statistical models. It is time-resolved, and only requires defining one parameter, namely the percentile defining what a *recurrence* is (see Text S1). In the future, the same approach may be extended to study lagged co-recurrence, which would allow to make causality statements. As all approaches, our analysis also displays some caveats. One is the dependence of the quantitative results on the choice of geographical domain. The co-recurrence ratio uses information from the full geographical domain considered, and larger domains will contain information about atmospheric patterns which have little connection with the extremes of interest. Additionally, the theoretical grounding of the calculation of the co-recurrence ratio may pose some challenges to interpreting the results for those not familiar with dynamical systems theory.

To conclude compound cold–wet–windy extremes in North America and Europe are only partly governed by a single set of coherent atmospheric circulation patterns. This motivates further analyses focussing specifically on the statistics and drivers of these compound extremes.

Acknowledgments

The authors have no conflicts of interest nor financial conflicts related to this work.

Open Research

The ERA5 data used in this study is freely available from the Copernicus Climate Change service at:

https://cds.climate.copernicus.eu/cdsapp#!/dataset/reanalysis-era5-single-levels?tab=form

https://cds.climate.copernicus.eu/cdsapp#!/dataset/reanalysis-era5-pressure-levels?tab=form

References

Brunner, M.I., Furrer, R. *and* Favre, A.-C. *(*2019*)* Modeling the spatial dependence of floods using the Fisher copula. *Hydrology and Earth System Sciences, 23,* 107–124. https://doi.org/10.5194/hess-23-107-2019

Cellitti, M. P., Walsh, J. E., Rauber, R. M., & Portis, D. H. (2006). Extreme cold air outbreaks over the United States, the polar vortex, and the large-scale circulation. *Journal of Geophysical Research: Atmospheres*, *111*(D2).

De Luca, P., Messori, G., Pons, F. M., & Faranda, D. (2020a). Dynamical systems theory sheds new light on compound climate extremes in Europe and Eastern North America. *Quarterly Journal of the Royal Meteorological Society*, *146*(729), 1636-1650.

De Luca, P., Messori, G., Faranda, D., Ward, P. J., Comou, D. (2020b) Compound warm-dry and cold-wet events over the Mediterranean. *Earth System Dynamics*, doi: 10.5194/esd-11-793-2020

Donat, M. G., Leckebusch, G. C., Pinto, J. G., & Ulbrich, U. (2010). Examination of wind storms over Central Europe with respect to circulation weather types and NAO phases. *International Journal of Climatology*, *30*(9), 1289-1300.

Faranda, D., Messori, G., and Vannitsem, S. (2019) Attractor dimension of time-averaged climate observables: insights from a low-order ocean-atmosphere model, *Tellus A, 71*, 1–11.

Faranda, D., Messori, G., & Yiou, P. (2020a). Diagnosing concurrent drivers of weather extremes: application to warm and cold days in North America. *Climate Dynamics*, *54*(3), 2187-2201.

Faranda, D., Vrac, M., Yiou, P., Jézéquel, A., & Thao, S. (2020b). Changes in future synoptic circulation patterns: Consequences for extreme event attribution. *Geophysical Research Letters*, 47, e2020GL088002. https://doi.org/10.1029/2020GL088002

Genton, M. G., Padoan, S. A., & Sang, H. (2015). Multivariate max-stable spatial processes. *Biometrika*, *102*(1), 215-230.

Gómara, I., Rodríguez-Fonseca, B., Zurita-Gotor, P., & Pinto, J. G. (2014). On the relation between explosive cyclones affecting Europe and the North Atlantic Oscillation. *Geophysical Research Letters*, *41*(6), 2182-2190.

Grotjahn, R.*, et al. (*2015*),* North American extreme temperature events and related large scale meteorological patterns: A review of statistical methods, dynamics, modeling, and trends, *Clim. Dyn.*, 1–34.

Hanley, J., & Caballero, R. (2012). The role of large-scale atmospheric flow and Rossby wave breaking in the evolution of extreme windstorms over Europe. *Geophysical Research Letters*, *39*(21).

Harnik, N., Messori, G., Caballero, R., & Feldstein, S. B. (2016). The circumglobal North American wave pattern and its relation to cold events in eastern North America. *Geophysical Research Letters*, *43*(20), 11-015.

Haylock, M. R., & Goodess, C. M. (2004). Interannual variability of European extreme winter rainfall and links with mean large-scale circulation. *International Journal of Climatology*, *24*(6), 759-776.

Hersbach, H., Bell, B., Berrisford, P., Hirahara, S., Horányi, A., Muñoz-Sabater, J., ... & Thépaut, J. N. (2020). The ERA5 global reanalysis. *Quarterly Journal of the Royal Meteorological Society*, *146*(730), 1999-2049.

Hillier, J. K., & Dixon, R. S. (2020). Seasonal impact-based mapping of compound hazards. *Environmental Research Letters*, *15*(11), 114013.

Lau, W. K., & Kim, K. M. (2012). The 2010 Pakistan flood and Russian heat wave: Teleconnection of hydrometeorological extremes. *Journal of Hydrometeorology*, *13*(1), 392-403.

Laurila, T. K., Gregow, H., Cornér, J., & Sinclair, V. A. (2021). Characteristics of extratropical cyclones and precursors to windstorms in northern Europe. *Weather and Climate Dynamics*, *2*(4), 1111-1130.

Lee, M. Y., C. C. Hong, *and* H. H. Hsu *(*2015*)*, Compounding effects of warm sea surface temperature and reduced sea ice on the extreme circulation over the extratropical North Pacific and North America during the 2013–2014 boreal winter, *Geophys. Res. Lett.*, *42*, 1612–1618.

Leeding, R., Riboldi, J., Messori, G. (2022) On Pan-Atlantic cold, wet and windy compound extremes, *Wea. Clim. Extr.*, 100524.

Liu, Y. R., Li, Y. P., Yang, X., Huang, G. H., & Li, Y. F. (2021). Development of an integrated multivariate trend-frequency analysis method: Spatial-temporal characteristics of climate extremes under global warming for Central Asia. *Environmental Research*, *195*, 110859.

Loikith, P. C., and A. J. Broccoli (2014), The influence of recurrent modes of climate variability on the occurrence of winter and summer extreme temperatures over North America, *Journal of Climate*, *27*(4), 1600–1618.

Lucarini, V., Faranda, D., de Freitas, J. M. M., Holland, M., Kuna, T., Nicol, M., ... & Vaienti, S. (2016). *Extremes and recurrence in dynamical systems*. John Wiley & Sons, London.

Lunt, T., Jones, A. W., Mulhern, W. S., Lezaks, D. P., & Jahn, M. M. (2016). Vulnerabilities to agricultural production shocks: An extreme, plausible scenario for assessment of risk for the insurance sector. *Climate Risk Management*, *13*, 1-9.

Matthias, V., & Kretschmer, M. (2020). The influence of stratospheric wave reflection on North American cold spells. *Monthly Weather Review*, *148*(4), 1675-1690.

Messori, G., & Caballero, R. (2015). On double Rossby wave breaking in the North Atlantic. *Journal of Geophysical Research: Atmospheres*, *120*(21), 11-129.

Messori, G., Caballero, R., & Gaetani, M. (2016). On cold spells in North America and storminess in western Europe. *Geophysical Research Letters*, *43*(12), 6620-6628.

Messori, G., Davini, P., Alvarez-Castro, M. C., Pausata, F. S., Yiou, P., & Caballero, R. (2019). On the low-frequency variability of wintertime Euro-Atlantic planetary wave-breaking. *Climate Dynamics*, *52*(3), 2431-2450.

Messori, G. and Faranda, D. (2021). Technical note: Characterising and comparing different palaeoclimates with dynamical systems theory. *Climate of the Past*, *17*, 545–563, https://doi.org/10.5194/cp-17-545-2021.

Messori, G., Kretschmer, M., Lee, S. H., and Matthias, V. (2022). Stratospheric Wave Reflection Events Modulate North American Weather Regimes and Cold Spells, *Weather and Climate Dynamics Discussion*, https://doi.org/10.5194/wcd-2022-18.

Naveau, P., Nogaj, M., Ammann, C., Yiou, P., Cooley, D., & Jomelli, V. (2005). Statistical methods for the analysis of climate extremes. *Comptes Rendus Geoscience*, *337*(10-11), 1013-1022.

Oesting, M. *and* Stein, A. *(*2018*)* Spatial modeling of drought events using max-stable processes. *Stochastic Environmental Research and Risk Assessment*, *32,* 63–81.

Owen, L. E., Catto, J. L., Stephenson, D. B., & Dunstone, N. J. (2021). Compound precipitation and wind extremes over Europe and their relationship to extratropical cyclones. *Weather and Climate Extremes*, 100342.

Palmer, T. *(*2014*)*, Record-breaking winters and global climate change, *Science*, *344(*6186*)*, 803–804.

Smith, E. T., & Sheridan, S. C. (2018). The characteristics of extreme cold events and cold air outbreaks in the eastern United States. *International Journal of Climatology*, *38*, e807-e820.

Tavakol, A., Rahmani, V., & Harrington Jr, J. (2020). Probability of compound climate extremes in a changing climate: A copula-based study of hot, dry, and windy events in the central United States. *Environmental Research Letters*, *15*(10), 104058.

Towler, E., Llewellyn, D., Prein, A., & Gilleland, E. (2020). Extreme-value analysis for the characterization of extremes in water resources: A generalized workflow and case study on New Mexico monsoon precipitation. *Weather and Climate Extremes*, *29*, 100260.

van Oldenborgh, G.J., Stephenson, D.B., Sterl, A., Vautard, R., Yiou, P., Drijfhout, S.S., von Storch, H. *and* van den Dool, H. *(*2015*)* Drivers of the 2013/14 winter floods in the UK. *Nature Climate Change, 5, 490–491.* *https://doi.org/10.1038/nclimate2612*

Vogel, J., Rivoire, P., Deidda, C., Rahimi, L., Sauter, C. A., Tschumi, E., ... & Zscheischler, J. (2021). Identifying meteorological drivers of extreme impacts: an application to simulated crop yields. *Earth system dynamics*, *12*(1), 151-172.

Zscheischler, J., Westra, S., Van Den Hurk, B. J., Seneviratne, S. I., Ward, P. J., Pitman, A., ... & Zhang, X. (2018). Future climate risk from compound events. *Nature Climate Change*, *8*(6), 469-477.